

DTIC FILE COPY

AFGL-TR-87-0080
ENVIRONMENTAL RESEARCH PAPERS, NO. 989

13

AD-A184 343

Microwave Refractive Index Structure Function Profiles (C_n^2) Measured From a Small Aircraft

JAMES F. MORRISSEY
YUTAKA IZUMI
OWEN R. COTE

DTIC
ELECTE
SEP 01 1987
S **D**



5 March 1987



Approved for public release; distribution unlimited.



ATMOSPHERIC SCIENCES DIVISION

PROJECT 6670

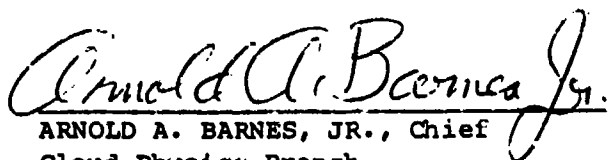
AIR FORCE GEOPHYSICS LABORATORY

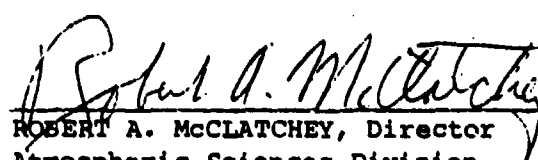
HANSCOM AFB, MA 01731

87 9 1 025

"This technical report has been reviewed and is approved for publication"

FOR THE COMMANDER


ARNOLD A. BARNES, JR., Chief
Cloud Physics Branch


ROBERT A. McCLATCHEY, Director
Atmospheric Sciences Division

This document has been reviewed by the ESD Public Affairs Office (PA) and is releasable to the National Technical Information Service (NTIS).

Qualified requestors may obtain additional copies from the Defense Technical Information Center. All others should apply to the National Technical Information Service.

If your address has changed, or if you wish to be removed from the mailing list, or if the addressee is no longer employed by your organization, please notify AFGL/DAA/LYC Hanscom AFB, MA 01731-5000. This will assist us in maintaining a current mailing list.

UNCLASSIFIED

SECURITY CLASSIFICATION OF THIS PAGE

AD-8184-343

REPORT DOCUMENTATION PAGE

1a. REPORT SECURITY CLASSIFICATION Unclassified			1b. RESTRICTIVE MARKINGS						
2a. SECURITY CLASSIFICATION AUTHORITY			3. DISTRIBUTION/AVAILABILITY OF REPORT Approved for public release; distribution unlimited.						
2b. DECLASSIFICATION/DOWNGRADING SCHEDULE									
4. PERFORMING ORGANIZATION REPORT NUMBER(S) AFGL-TR-87-0080 ADLERP, No. 969			5. MONITORING ORGANIZATION REPORT NUMBER(S)						
6a. NAME OF PERFORMING ORGANIZATION Air Force Geophysics Laboratory		6b. OFFICE SYMBOL (If applicable) LYC		7a. NAME OF MONITORING ORGANIZATION					
6c. ADDRESS (City, State and ZIP Code) Hanscom AFB Massachusetts 01731-5000			7b. ADDRESS (City, State and ZIP Code)						
8a. NAME OF FUNDING/SPONSORING ORGANIZATION		8b. OFFICE SYMBOL (If applicable)		9. PROCUREMENT INSTRUMENT IDENTIFICATION NUMBER					
8c. ADDRESS (City, State and ZIP Code)			10. SOURCE OF FUNDING NOS.						
			<table border="1"> <tr> <td>PROGRAM ELEMENT NO. 62101F</td> <td>PROJECT NO. 6670</td> <td>TASK NO. 14</td> <td>WORK UNIT NO. 07</td> </tr> </table>			PROGRAM ELEMENT NO. 62101F	PROJECT NO. 6670	TASK NO. 14	WORK UNIT NO. 07
PROGRAM ELEMENT NO. 62101F	PROJECT NO. 6670	TASK NO. 14	WORK UNIT NO. 07						
11. TITLE (Include Security Classification) Microwave Refractive Index Structure Function Profiles (C_n^2) Measured From a (Contd)									
12. PERSONAL AUTHOR(S) Morrissey, James F., Izumi, Yutaka, and Cote, Owen R.									
13a. TYPE OF REPORT Scientific, Final		13b. TIME COVERED FROM 1985 TO 1987		14. DATE OF REPORT (Yr., Mo., Day) 1987 March 5					
				15. PAGE COUNT 30					
16. SUPPLEMENTARY NOTATION									
17. COSATI CODES			18. SUBJECT TERMS (Continue on reverse if necessary and identify by block number)						
FIELD	GROUP	SUB. GR.	Refractive index structure function, Refractometers, and Atmospheric refraction.						
19. ABSTRACT (Continue on reverse if necessary and identify by block number)									
<p>Measurements of the microwave refractive index structure function (C_n^2) obtained with a microwave refractometer on a small aircraft are presented. Thin layers (< 300 m) of highly enhanced C_n^2 were observed on several flights, usually associated with an inversion. Results from two refractometers about 4 m apart are shown for several flights. The double measurements are discussed from the point of view of the validity of the measurements themselves.</p> <p><i>(negated, included)</i></p>									
20. DISTRIBUTION/AVAILABILITY OF ABSTRACT UNCLASSIFIED/UNLIMITED <input type="checkbox"/> SAME AS RPT. <input checked="" type="checkbox"/> DTIC USERS <input type="checkbox"/>			21. ABSTRACT SECURITY CLASSIFICATION Unclassified						
22a. NAME OF RESPONSIBLE INDIVIDUAL James F. Morrissey			22b. TELEPHONE NUMBER (Include Area Code) (617) 377-2943		22c. OFFICE SYMBOL LYC				

DD FORM 1473, 83 APR

EDITION OF 1 JAN 73 IS OBSOLETE.

UNCLASSIFIED
SECURITY CLASSIFICATION OF THIS PAGE

Unclassified

SECURITY CLASSIFICATION OF THIS PAGE

11. Title (Contd)

Small Aircraft

Unclassified

SECURITY CLASSIFICATION OF THIS PAGE

Contents

1. INTRODUCTION	1
2. DESCRIPTION OF MEASUREMENT	2
2.1 Measurement Technique	2
2.2 Flight Technique	3
2.3 Measurement Sensors/System	4
3. DATA PROCESSING	7
4. DISCUSSION	11
5. CONCLUSIONS	13
REFERENCES	15
APPENDIX A	17

Accession For		1	
NTIS	CRA&I	<input checked="" type="checkbox"/>	2
DTIC	TAB	<input type="checkbox"/>	2
Unannounced		<input type="checkbox"/>	3
Justification			4
By			7
Distribution /			11
Availability Codes			13
Dist	Avail and/or Special		15
A-1			17



Illustrations

1. Microwave Cavity Mounted on Strut of Cessna-172 Aircraft as Flown	4
2. Map Showing Local Area of Tests, Chatham, and General Flight Path	5
3. Block Diagram of Microwave Refractometer	6
4. Refractometers With Associated Computers and Recorders as Flown in Tests	7

Illustrations

5. Chart Showing Data Reduction Technique	8
6. Sample Power Density Distribution $\phi_n(k)$ for Flight of 25 September at 1618 EDT	8
7. C_n^2 Profile for Flight of 18 September at 1525 EDT With Temperature (T) and Dew Point Temperature (T_D) From Radiosonde Flight at 1510 EDT	9
8. Sequence of Dual C_n^2 Measurements From Flight of 26 September at 1434 EDT	10
9. Sample of Coherence and Phase Spectra From Flight of 26 September at 1434 EDT	10
10. Sampled Voltage Sequences From Both Refractometers From Flight of 25 September at 1125 EDT	12
A1. Measured C_n^2 Profile (18 Sept 0730) With T and T_D From Radiosonde Closest in Time	19
A2. Measured C_n^2 Profile (18 Sept 1525) With T and T_D From Radiosonde Closest in Time	19
A3. Measured C_n^2 Profile (19 Sept 0719) With T and T_D From Radiosonde Closest in Time	20
A4. Measured C_n^2 Profile (20 Sept 0741) With T and T_D From Radiosonde Closest in Time	20
A5. Measured C_n^2 Profile (20 Sept 1113) With T and T_D From Radiosonde Closest in Time	21
A6. Measured C_n^2 Profile (21 Sept 0747) With T and T_D From Radiosonde Closest in Time	21
A7. Measured C_n^2 Profile (24 Sept 0730) With T and T_D From Radiosonde Closest in Time	22
A8. Measured C_n^2 Profile (25 Sept 0653) With T and T_D From Radiosonde Closest in Time	22
A9. Measured C_n^2 Profile (25 Sept 0959) With T and T_D From Radiosonde Closest in Time	23
A10. Measured C_n^2 Profile (25 Sept 1626) With T and T_D From Radiosonde Closest in Time	23
A11. Measured C_n^2 Profile (26 Sept 0707) With T and T_D From Radiosonde	24
A12. Measured C_n^2 Profile (26 Sept 0707) With T and T_D From Radiosonde Closest in Time	24
A13. Measured C_n^2 Profile (26 Sept 0707) With T and T_D From Radiosonde	25
A14. Measured C_n^2 Profile (26 Sept 1434) With T and T_D From Radiosonde Closest in Time	25

Microwave Refractive Index Structure Function Profiles (C_n^2) Measured From a Small Aircraft

1. INTRODUCTION

In September 1985 a series of airplane flights were performed to obtain measurements of the microwave refractive index structure function (C_n^2) in and around inversion layers. This series had two goals associated with C_n^2 measurement: one was to provide evidence on the validity of the measurements themselves; the other was to provide information on the variation of C_n^2 in the first few km of the atmosphere. Of primary importance was the thickness and magnitude of any enhanced layers. The basic interest in the measurements of C_n^2 was to understand the performance of troposcatter radio performance. The magnitude and shape of enhanced layers strongly influence the performance of these radios and can dictate the strategy of making the C_n^2 measurements themselves.

The tests were carried out at Chatham, Mass. The C_n^2 measurements were obtained using a microwave refractometer with the sensing cavity mounted to the wing strut of a Cessna-172 aircraft. Supporting atmospheric data were obtained from a portable radiosonde system and from synoptic radiosondes. These radiosonde flights were taken at the National Weather Service (NWS) station at

(Received for Publication 3 March 1987)

Chatham. An earlier report¹ compared the measurement of radio ducts by the two radiosonde systems and the airborne refractometer.

2. DESCRIPTION OF MEASUREMENT

2.1 Measurement Technique

A time sequence of refractive index variation measurements $n(t_i)$ is obtained with a microwave refractometer mounted under the wing of an aircraft. This time sequence is converted to a power spectral density function ϕ_n by taking the fast Fourier transform (FFT) and dividing by the frequency separation

$$\phi_n(f_i) = A(f_i)^2 / \Delta f \quad (1)$$

where $A(f)$'s are the amplitude from a FFT and Δf is the width between frequencies (f_i).

Assuming the Taylor hypothesis to be valid, the time spectrum is then converted to a spatial spectrum by dividing by the average velocity of the air relative to the sensor:

$$\phi_n(k_i) = \phi_n(f_i) / V \quad (2)$$

where V is the velocity of air relative to the sensor, and k is the wavenumber.

These spectra are then used to calculate C_n^2 according to the $-5/3$ power law for three-dimensional turbulence in the inertial subrange given by Tatarski² and Wyngaard and LeMone.³

$$C_n^2 = 0.25 \phi_n(k) k^{-5/3} \quad (3)$$

On some flights, two refractometers were used, generating two time sequences of refractive index measurements $[n_1(t_i), n_2(t_i)]$. The coherence spectrum and phase spectrum for these time sequences were computed using

1. Morrissey, J., Izumi, Y., and Coté, O. (1986) Intercomparisons of Radiosondes and an Airborne Refractometer for Measuring Radio Ducts, AFGL-TR-86-0143, AD A175150.
2. Tatarski, V. L. (1961) Wave Propagation in a Turbulent Medium, McGraw-Hill, New York.
3. Wyngaard, J. C., and LeMone, M. A. (1980) Behavior of the refractive index structure parameter in the entraining convective boundary layer, J. Atmos. Sci. 37:1573-1585.

$$\text{Coh}(f) = \frac{\{[\phi_{n_1 n_2}(f)]^2 + [QD_{n_1 n_2}(f)]^2\}^{1/2}}{\phi_{n_1}(f) \phi_{n_2}(f)}$$

and

(4)

$$\text{Phase}(f) = \tan^{-1} \frac{QD_{n_1 n_2}(f)}{\phi_{n_1 n_2}(f)}.$$

where $\phi_{n_1 n_2}$ is the cospectrum of n_1 and n_2 .

$QD_{n_1 n_2}$ is the quadrature cospectrum of n_1 and n_2 , and

$\phi_{n_1} \phi_{n_2}$ are the power spectra of n_1 and n_2 .

2.2 Flight Technique

To obtain the necessary time sequence of refractive index measurements, the sensing cavity of a microwave refractometer was attached to the wing strut of a C-172 aircraft just below the leading edge of the aircraft wing (Figure 1). The aircraft was then flown at various altitudes, maintaining altitude, air speed, and direction as constant as possible. These level data gathering runs were at ~100 knots true air speed (TAS), lasted 5-1/2 min or more, and covered in excess of 10 miles. These runs were from about 5 miles south of the Chatham Weather Service Station over Monomoy Island to about 5 miles north of the station beside Orleans (Figure 2).

The flight levels were selected for several reasons. Usually, one level was at about 3 km to characterize the area well above the inversions, if any. If there were inversions, several levels were selected to be either just above, in, or just below the inversion. On some flights, one or more of these levels were repeated. Then, when time permitted, a series of low level runs were performed at typically 15, 30, 60, 120, and 240 m altitude. The selection of the flight levels was made using information transmitted to the aircraft from the radiosonde runs. In addition, each flight began with the aircraft spiralling up from the surface to 3 km, and data from this ascent was also used in selecting levels.

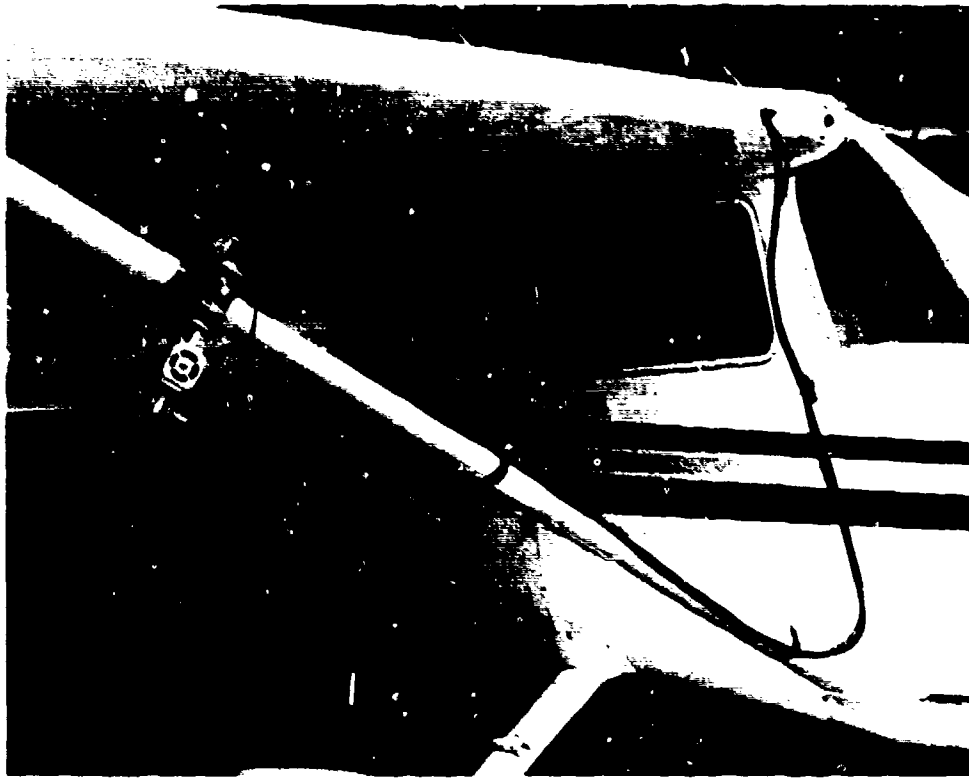


Figure 1. Microwave Cavity Mounted on Strut of Cessna-172 Aircraft as Flown

2.3 Measurement Sensors/System

The primary sensor is the microwave refractometer previously developed at the National Telecommunications and Information Sciences (NTIS) laboratory in Boulder, Colo.⁴ The refractometer is a single cavity Birnbaum type. Figure 3 is a simplified block diagram of the refractometer. The cavity is continuously driven by a signal that is centered on the resonant frequency of the cavity, has a 10 kHz sweep frequency, and causes a deviation of ± 40 kHz. The center frequency is made to track the resonant frequency of the cavity by feedback from a phase sensitive detector that offsets the voltage controlled oscillator (VCXO). The output of the VCXO is averaged and scaled to produce a digital output that is displayed on the front panel. This same digital output is passed through a

4. Thompson, M. C., Marler, F. E., and Allen, K. C. (1985) Measurement of the microwave structure constant profile, IEEE Trans. Antennas Propag. AP-28(No. 2):278-280.

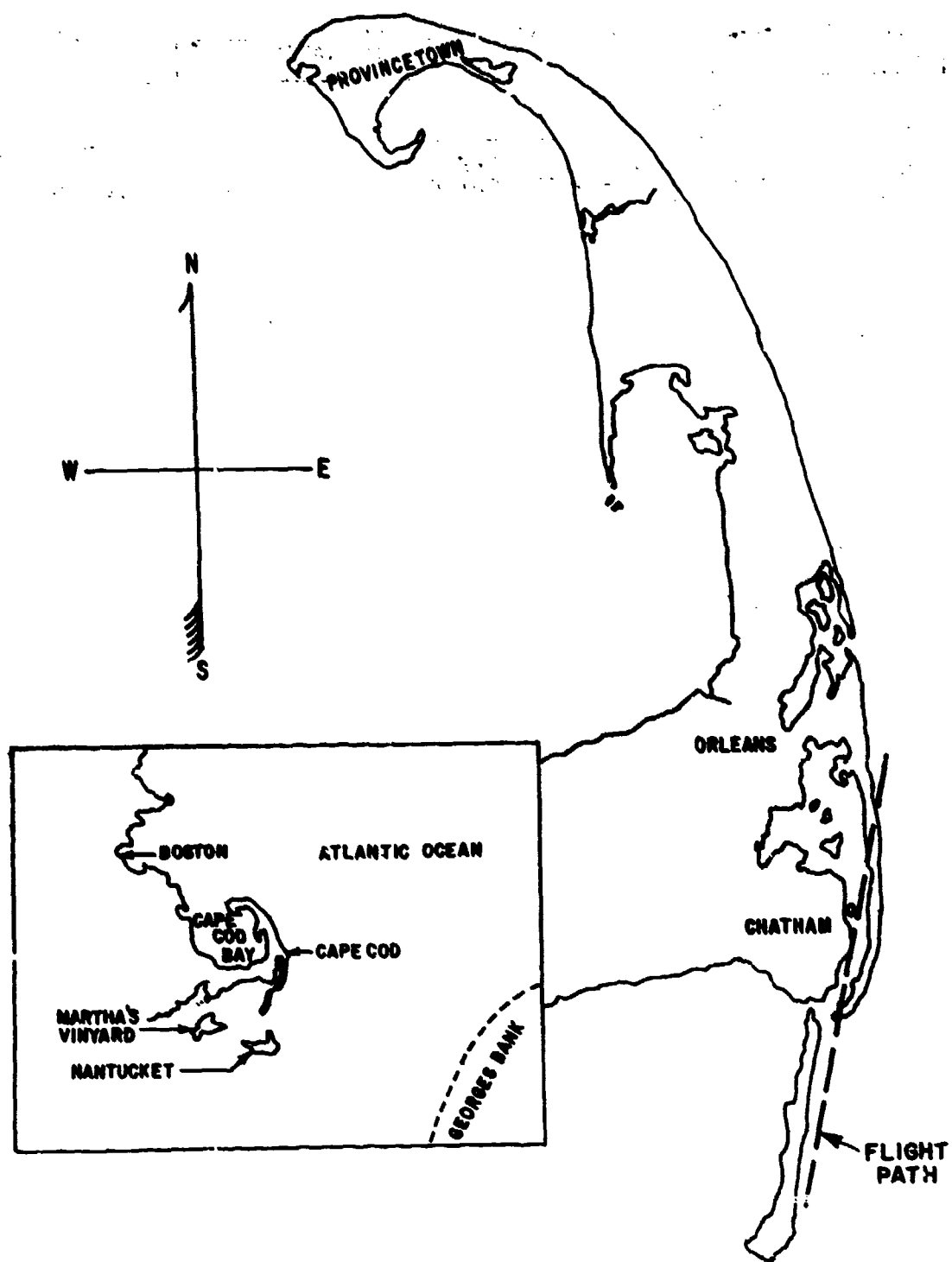


Figure 2. Map Showing Local Area of Tests, Chatham, and General Flight Path

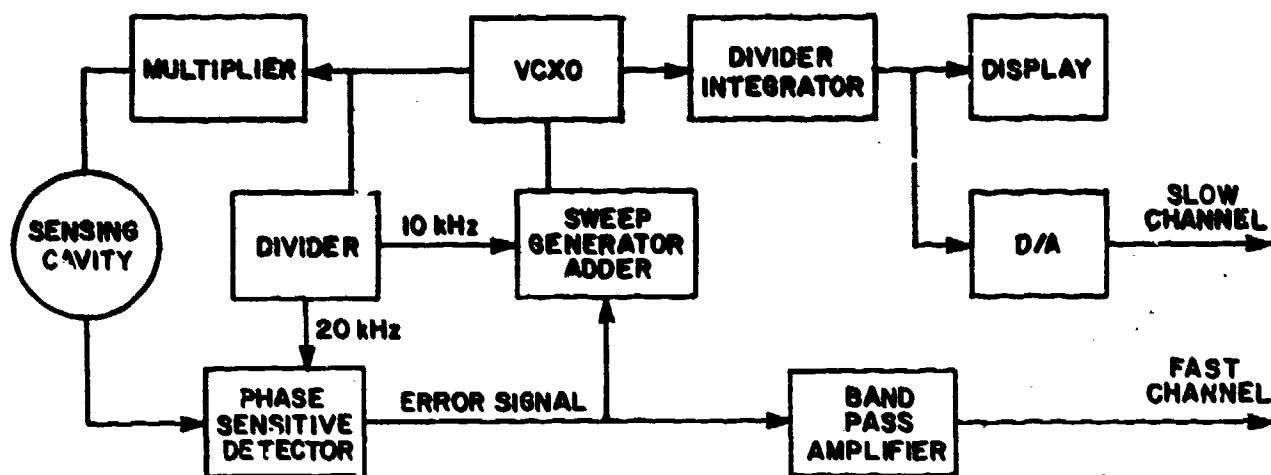


Figure 3. Block Diagram of Microwave Refractometer

digital-to-analog converter and represents one of the analog outputs. This channel has a sensitivity of 0.01 V/n units and an averaging time/update rate of 1 sec as flown. The second analog channel is obtained by taking the analog error voltage and passing it through a bandpass filter (1/100 to 10 cycles) amplifier. This channel, as flown, had a maximum sensitivity of 1.04 V/n units (1.28 V/n, refractometer No. 2) at a frequency of 2 cycles.

In addition to the refractometer, the air temperature was measured by a bead thermistor mounted just above the refractometer cavity, and pressure was measured inside the aircraft by a Rosemount Model 1201F1 pressure transducer.

A data system was designed for the C_n^2 measurements program (Figure 4). It consists of a Euromak C computer, manufactured by Dr. Weiss GMBH, that is used to control 12 A/D (12 bit) channels. Six channels are programmed to be sampled at a rate of two times per second and six channels are programmed for 64 times per second. Only two of the fast channels were used in this series. The system is under the control of an operator using a small NEC - PC8201A computer. The operator is allowed to input titles and observations of two types; one at the start of each flight or new tape, and another in between each data run. The first is used to give the location and general observations on the test and the atmosphere. The second is used to give specific data and observations associated with the upcoming data run (i. e., air speed, altitude, heading, location, visibility, and bumpiness) as well as additions and comments on the previous run. The data were stored on a nine-track magnetic tape recorder (Kennedy 9832) during these tests, but the system has since been modified to use a cassette style tape recorder (Kennedy 6455).



Figure 4. Refractometers With Associated Computers and Recorders as Flown in Tests

3. DATA PROCESSING

Figure 5 symbolically shows the data processing used to obtain each estimate of C_n^2 . Sixty-four seconds of the sampled high gain channel of the refractometer (4096 values) are detrended and converted to a frequency spectrum $\psi_n(f_i)$, which is then converted to a power density spectrum. This step required the removal of the frequency dependency, $\frac{1}{|G_f|}$, introduced by the pre-whitening filter in the refractometer. This frequency spectrum is converted to a wavenumber spectrum, $\phi_n(K_i)$, by dividing by the true air speed of the aircraft. A sample power density spectrum from the 25 September flight at 1618 EDT at Chatham is shown in Figure 6. This spectrum is then used to generate the estimate of C_n^2 by using the mean value of C_{ni}^2 calculated for each wavenumber corresponding to $i = 25$ to $i = 104$. These represent wavelengths from 30 to 130 m at an air speed of 51.4 m/sec (100 knots), which is representative of the speed in these flights.

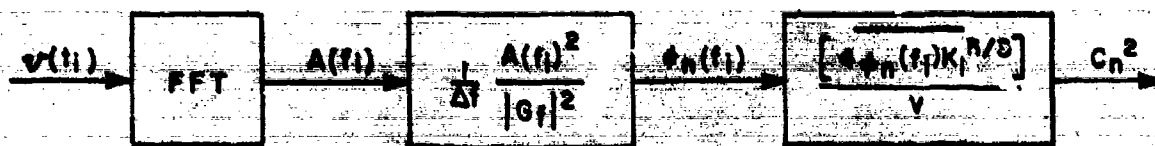


Figure 5. Chart Showing Data Reduction Technique

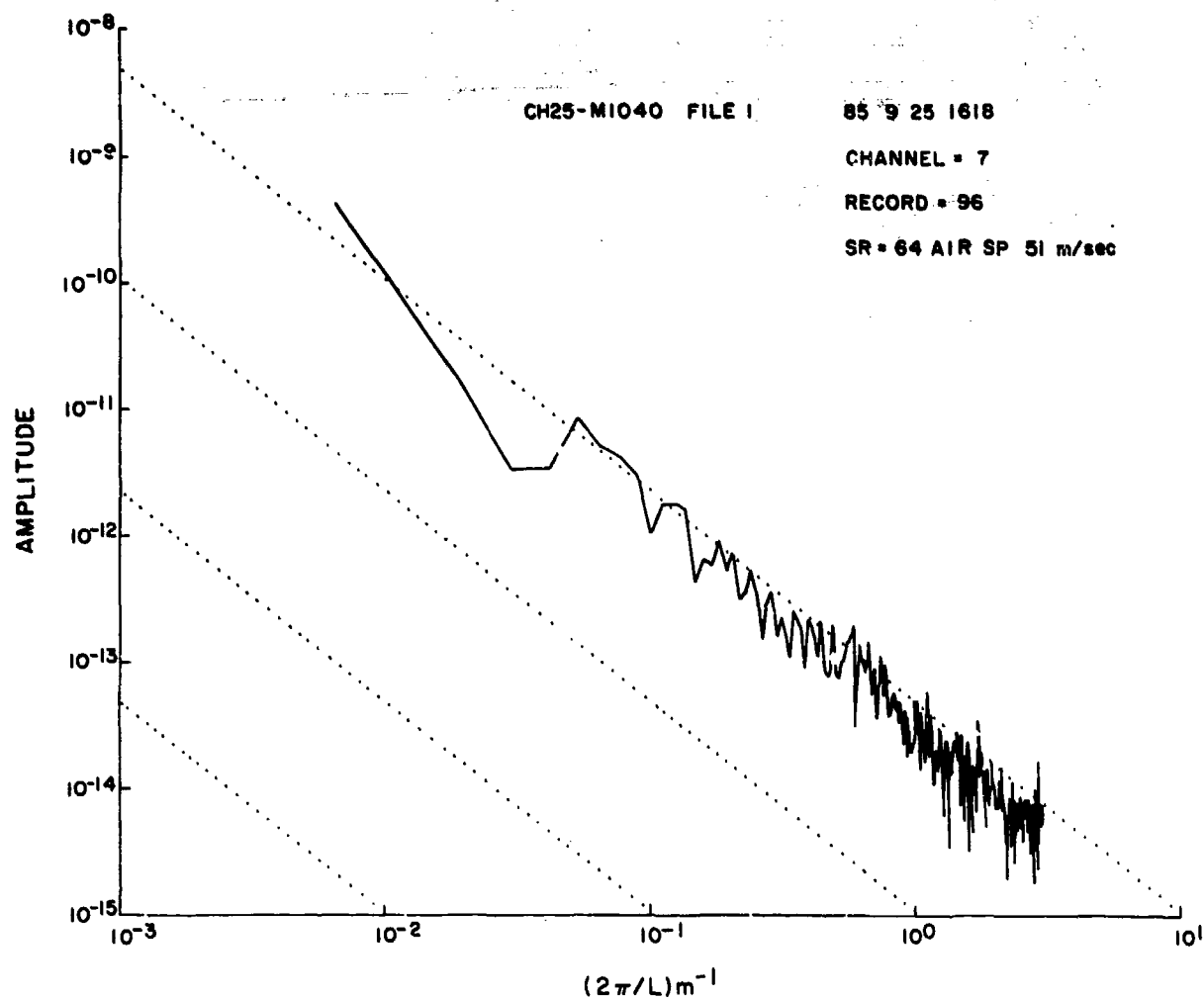


Figure 6. Sample Power Density Distribution $\phi_n(k)$ for Flight of 25 September at 1618 EDT

During each of these C_n^2 estimates, 64 sec of data, the aircraft moves about 3 km. Each level run contained five such segments. Figure 7 shows the C_n^2 results from the flight on 18 September at 1525 EDT. At each level the mean, usually of five values, is shown and the standard deviation is shown as bars. The temperature and dew point profiles from the radiosonde closest in time to the aircraft flight are also shown.

On those flights where two refractometers were flown, the sampled data was processed from each refractometer separately as described above. This provides time series of dual measurements of C_n^2 where the refractometers are 4.25 m apart. Figure 8 shows the C_n^2 results from the 26 September flight at 1434 EDT. The results are in the order taken, with vertical lines used to separate areas of constant altitude. In addition, the two sets of sampled analog data were used to generate coherence spectra and phase spectra. This was accomplished by first calculating the cospectra and quadrature spectra in a manner analogous to that shown in Figure 5. Figure 9 shows a typical plot of these spectra from the flight of 25 September at 1618 EDT.

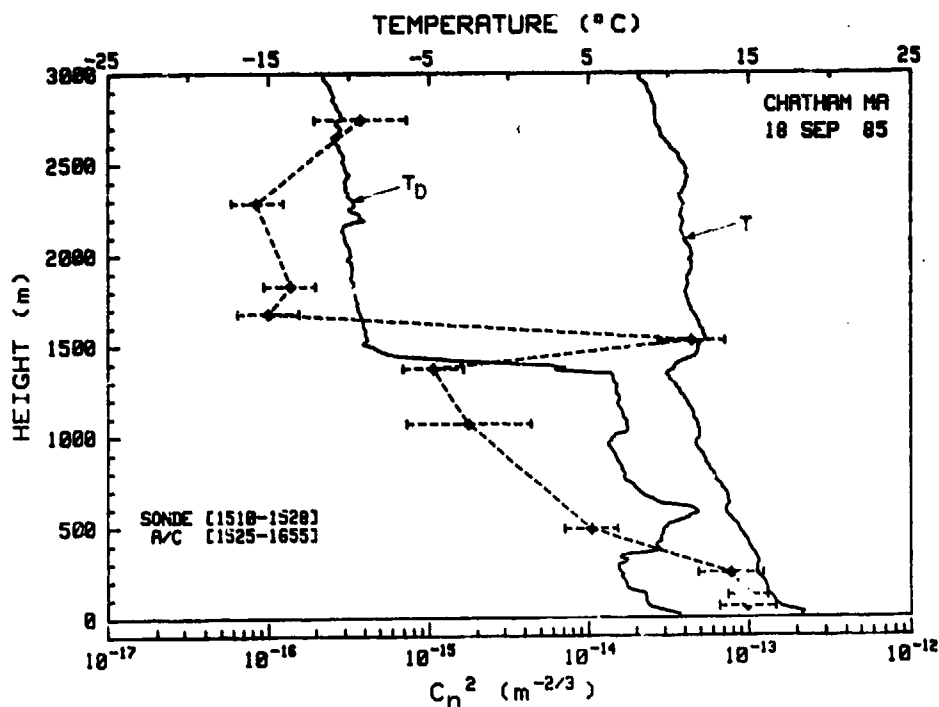


Figure 7. C_n^2 Profile for Flight of 18 September at 1525 EDT With Temperature (T) and Dew Point Temperature (T_D) From Radiosonde Flight at 1510 EDT

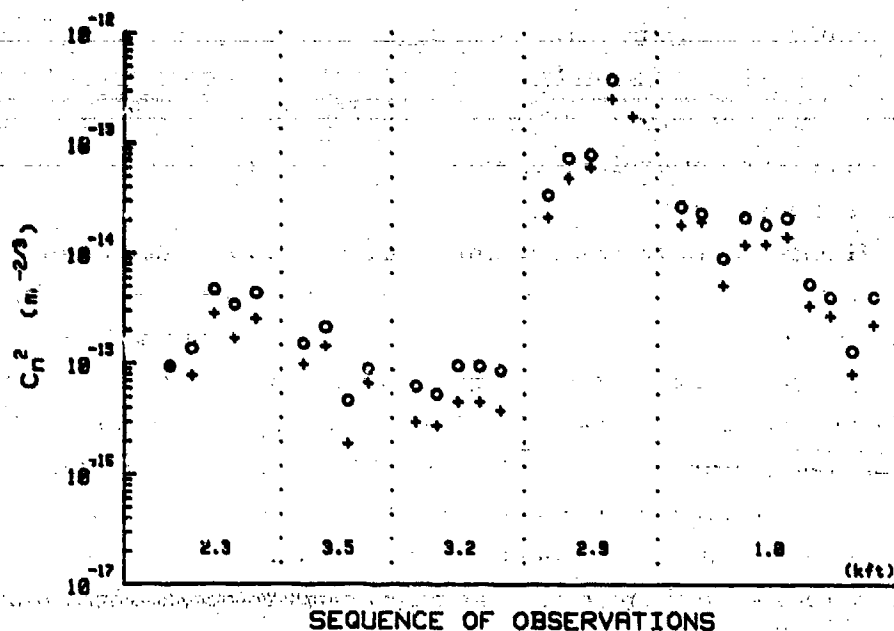


Figure 8. Sequence of Dual C_n^2 Measurements From Flight of 26 September at 1434 EDT

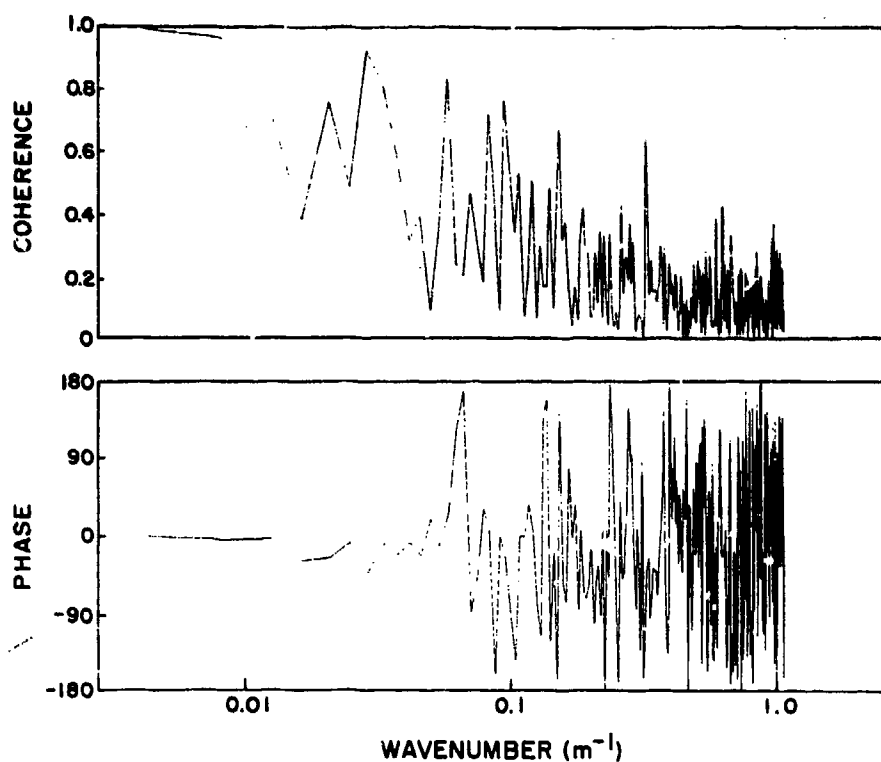


Figure 9. Sample of Coherence and Phase Spectra From Flight of 26 September at 1434 EDT

4. DISCUSSION

Two types of information were gained from the program; information on the measurement technique, and data on the distribution of C_n^2 in the lowest couple of km of the atmosphere.

The use of two refractometers demonstrated the high degree of repeatability of the technique. This can be seen in Figure 10, which shows the digitized voltage sequences from a couple of data blocks (512 samples, 8 sec) from the flight on 25 September. This high degree of repeatability is also evident in the five figures in Appendix A that show the mean C_n^2 values from two refractometers (Figures A7, A9, A11, A12, and A13). These figures show a consistent offset in the two measurements. This offset is not unexpected in that time and circumstances prevented an absolute calibration of the second refractometer. This agreement is also evident when we look at the individual C_n^2 values obtained during each level portion of flight (Figure 8). Again, the offset between the refractometers is evident.

The final way that the dual refractometers were compared was by coherence and phase spectra of the two signals. Figure 9 shows the signals to be well correlated at wavelengths longer than 25 m and to have a zero degree phase shift between refractometers. At shorter wavelengths, the correlation deteriorates and the phase shift is no longer zero until, at wavelengths of less than 5 m, the picture is chaotic. This behavior is expected for two sensors separated by 4.25 m.⁵ The signals should be well correlated with zero phase shift until the wavelength is about four times the separation, or 20 m.

The measured values of C_n^2 range from a high of $3 \times 10^{-13} \text{ m}^{-2/3}$ to a low of $5 \times 10^{-17} \text{ m}^{-2/3}$. Of more importance to understanding the performance of troposcatter radios is the large observed vertical gradients. One of the largest gradients can be seen at about 1600 m on the second flight of 18 September (Figure A2). C_n^2 goes from 3×10^{-14} to $9 \times 10^{-17} \text{ m}^{-2/3}$, a ratio of 300 to 1, in a vertical separation of 150 m.

On several flights, we see a correspondence between the typical inversion, rising air temperature and falling dew point temperature, and a sharp decrease in C_n^2 with height (Figures A2, A3, A4, A6, A10, and A14). This decrease, at times, exactly corresponds to the decrease in dew point, while, in other cases, it is displaced vertically upward a couple of hundred meters. Often there is also

5. Priestley, J. T., and Hill, R. J. (1985) Measuring high-frequency humidity, temperature and radio refractive index in the surface layer, J. Atmos. and Oceanic Technol. 2:233-251.

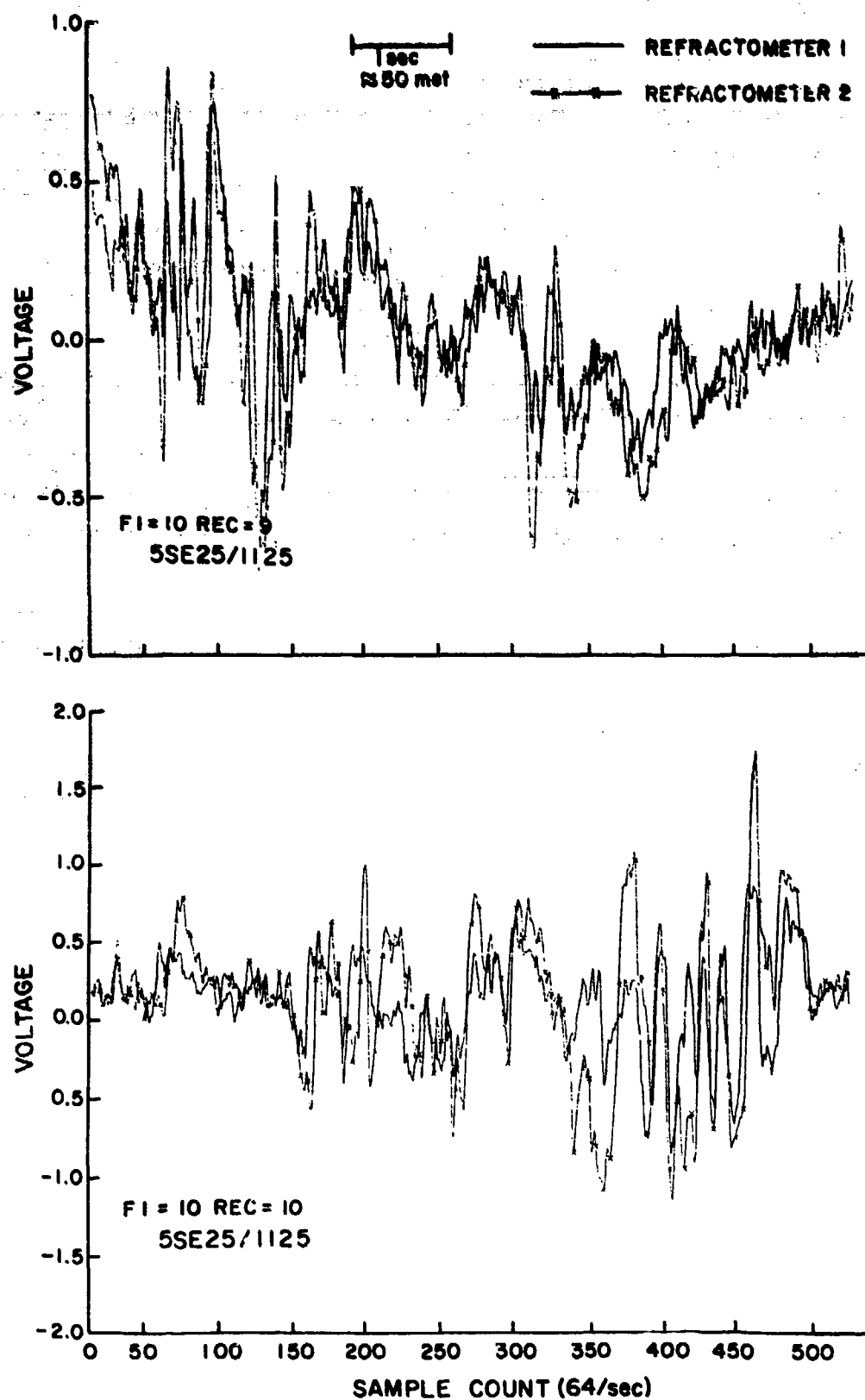


Figure 10. Sampled Voltage Sequences From Both Refractometers From Flight of 25 September at 1125 EDT

a sharp increase in C_n^2 with increasing height just below the inversion. This results in an enhanced layer of C_n^2 right at, and sometimes slightly above, the inversion where the ratio inside the layer to outside is typically from 40 to 100 times (Figures A2, A6, A10, and A14).

On those days where there were low level runs below 200 m, we see the enhanced levels of C_n^2 associated with surface friction, $1 \times 10^{-13} \text{ m}^{-2/3}$, which usually falls off to about $1 \times 10^{-15} \text{ m}^{-2/3}$ by 500 m. This decrease is often not monotonic, but shows a pronounced increase with height in the first 100 m. This increase with height may be an artifact of data processing, since the altitude is less than some of the wavelengths used in calculating C_n^2 .

5. CONCLUSIONS

The results provide strong evidence that these measurements, obtained from a refractometer mounted on a small aircraft, can provide useful information on the small scale fluctuations of n . This can be used in the study of the refractive index structure function that influences many modern radar and propagation systems.

Several cases showed layers of very limited vertical extent ($< 300 \text{ m}$), where C_n^2 increased by 40 to 300 times. The sharp layers were usually associated with a temperature inversion and an associated sharp decrease in water vapor. The shallowness of these layers might cause them to be misrepresented in any experiment with a vertical sampling interval greater than 200 m. The shape and position of the layers could be critical to understanding the performance of various radars (airborne surveillance radars and synthetic aperture radars) and communication systems, i.e., the shifting of the layers by about 400 m could increase/decrease delay spread on a troposcatter radio link by several times.

References

1. Morrissey, J., Izumi, Y., and Côté, O. (1986) Intercomparisons of Radiosondes and an Airborne Refractometer for Measuring Radio Ducts, AFGL-TR-86-0143, AD A175150.
2. Tartarski, V.L. (1961) Wave Propagation in a Turbulent Medium, McGraw-Hill, New York.
3. Wyngaard, J. C., and LeMone, M. A. (1980) Behavior of the refractive index structure parameter in the entraining convective boundary layer, J. Atmos. Sci. 37:1573-1585.
4. Thompson, M. C., Marler, F. E., and Allen, K. C. (1985) Measurement of the microwave structure constant profile, IEEE Trans. Antennas Propag. AP-33(No. 2):278-280.
5. Priestley, J. T., and Hill, R. J. (1985) Measuring high-frequency humidity, temperature and radio refractive index in the surface layer, J. Atmos. and Oceanic Technol. 2:233-251.

Appendix A

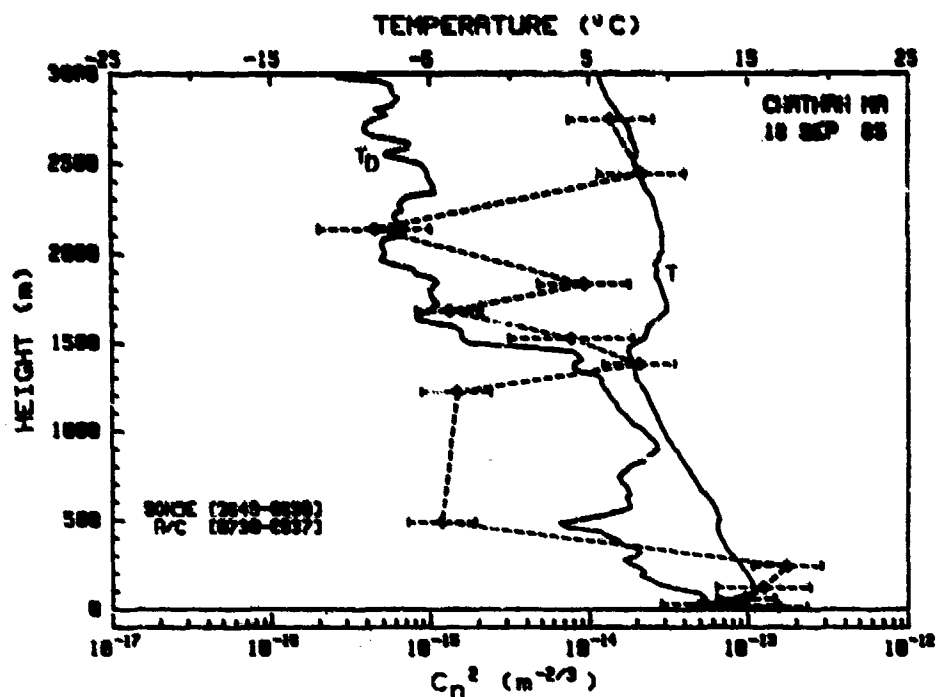


Figure A1. Measured C_n^2 Profile (18 Sept 0730) With T and T_D From Radiosonde Closest in Time

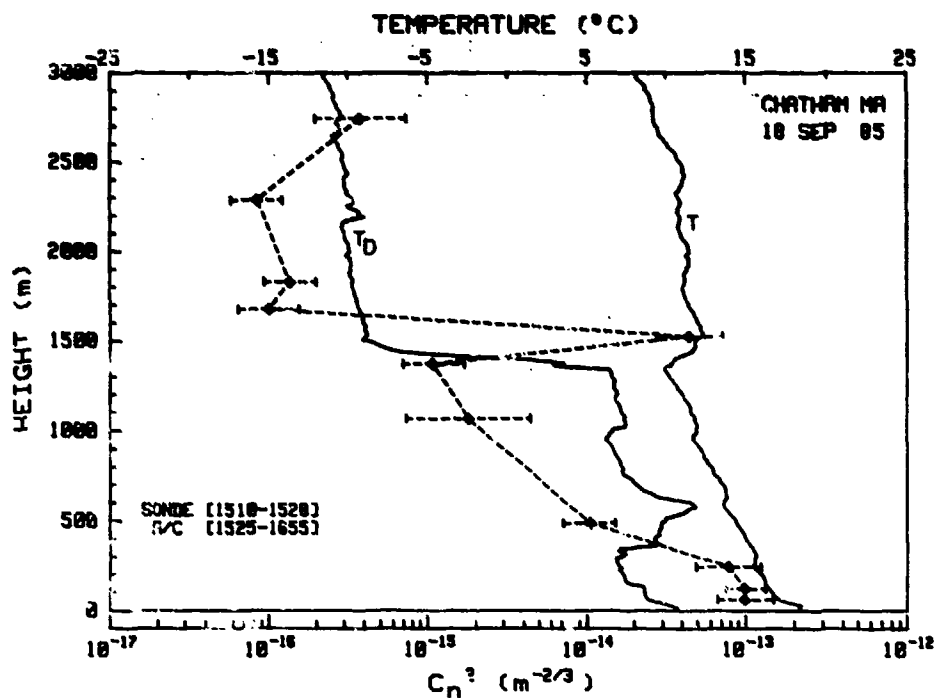


Figure A2. Measured C_n^2 Profile (18 Sept 1525) With T and T_D From Radiosonde Closest in Time

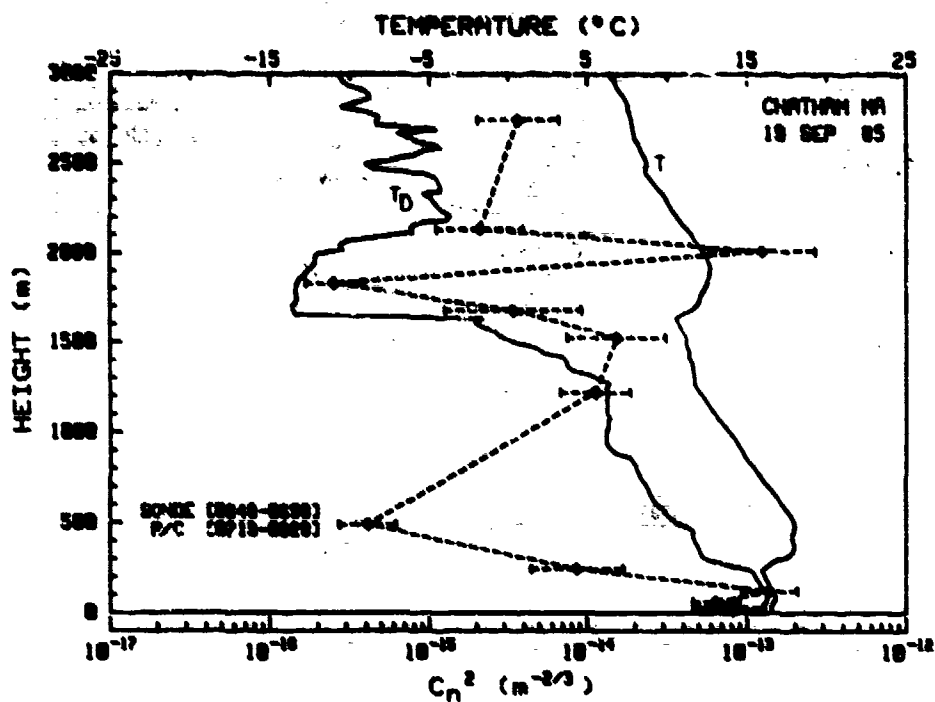


Figure A3. Measured C_n^2 Profile (19 Sept 0719) With T and T_D From Radiosonde Closest in Time

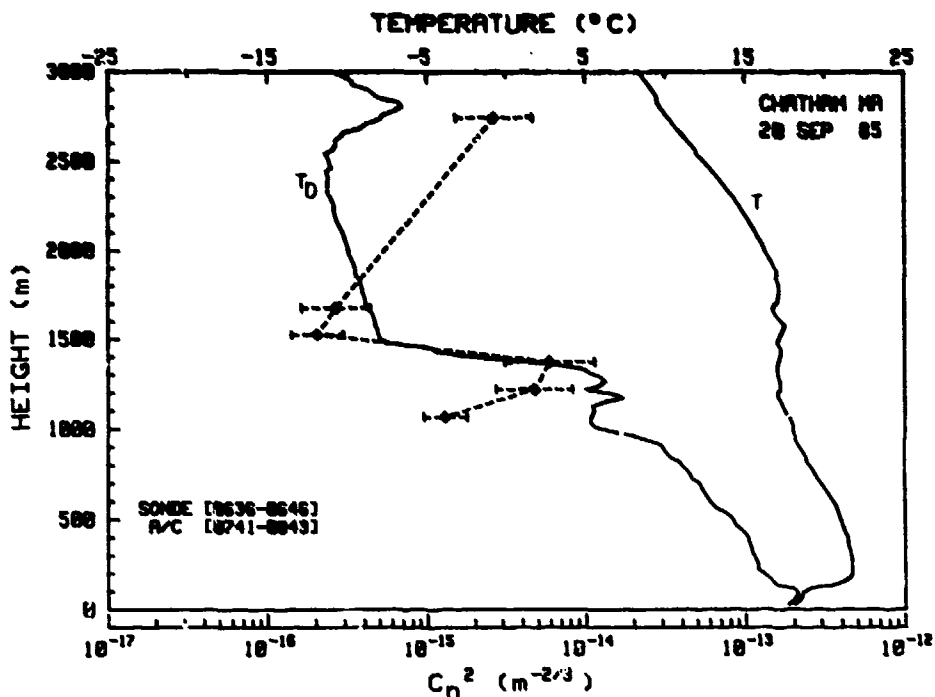


Figure A4. Measured C_n^2 Profile (20 Sept 0741) With T and T_D From Radiosonde Closest in Time

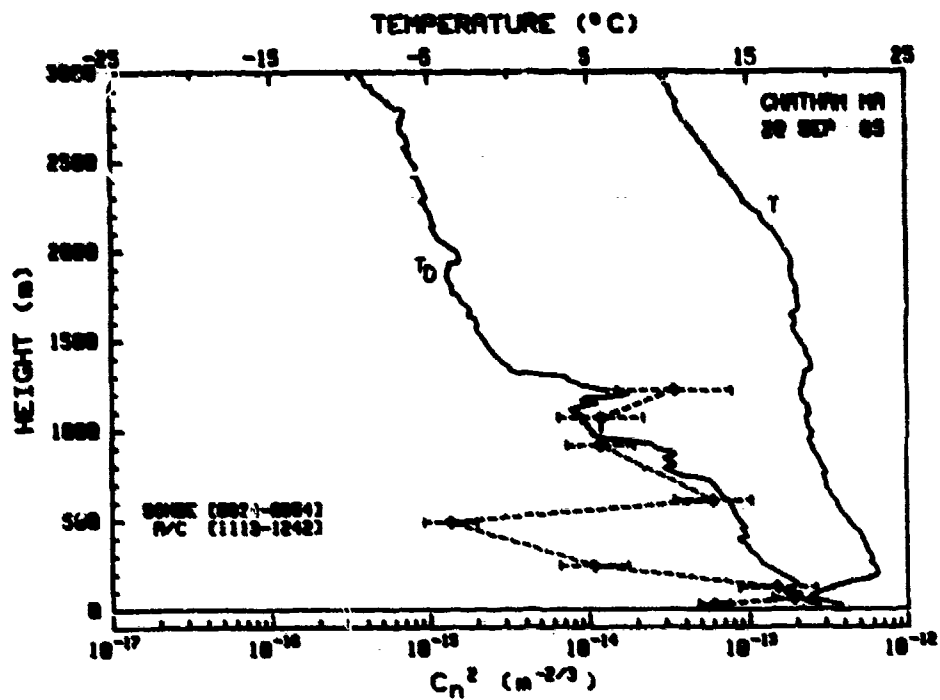


Figure A5. Measured C_n^2 Profile (20 Sept 1113) With T and T_D From Radiosonde Closest in Time

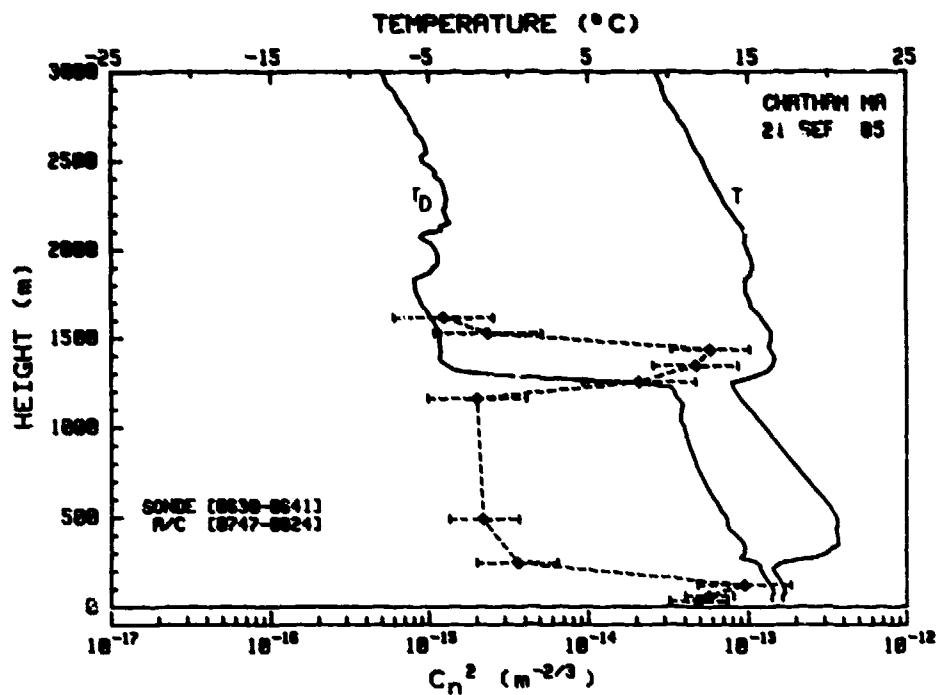


Figure A6. Measured C_n^2 Profile (21 Sept 0747) With T and T_D From Radiosonde Closest in Time

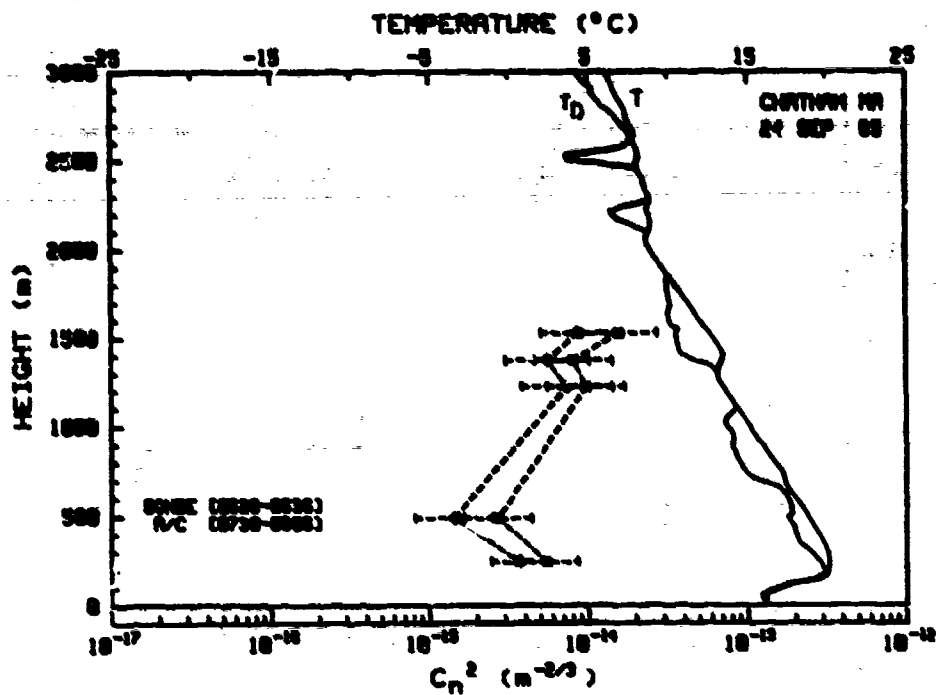


Figure A7. Measured C_n^2 Profile (24 Sept 0730) With T and T_D From Radiosonde Closest in Time

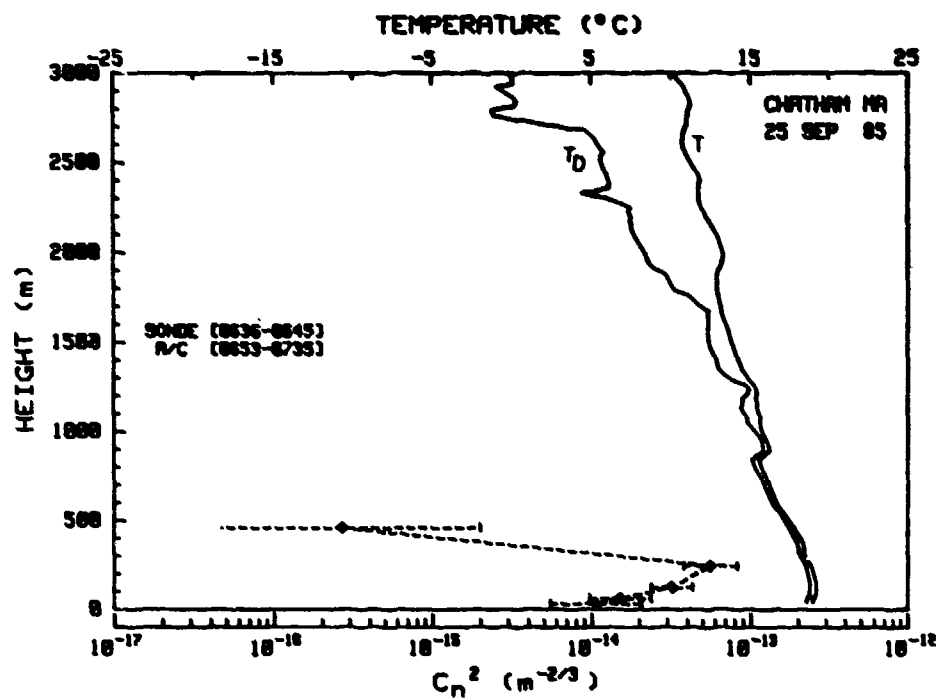


Figure A8. Measured C_n^2 Profile (25 Sept 0653) With T and T_D From Radiosonde Closest in Time

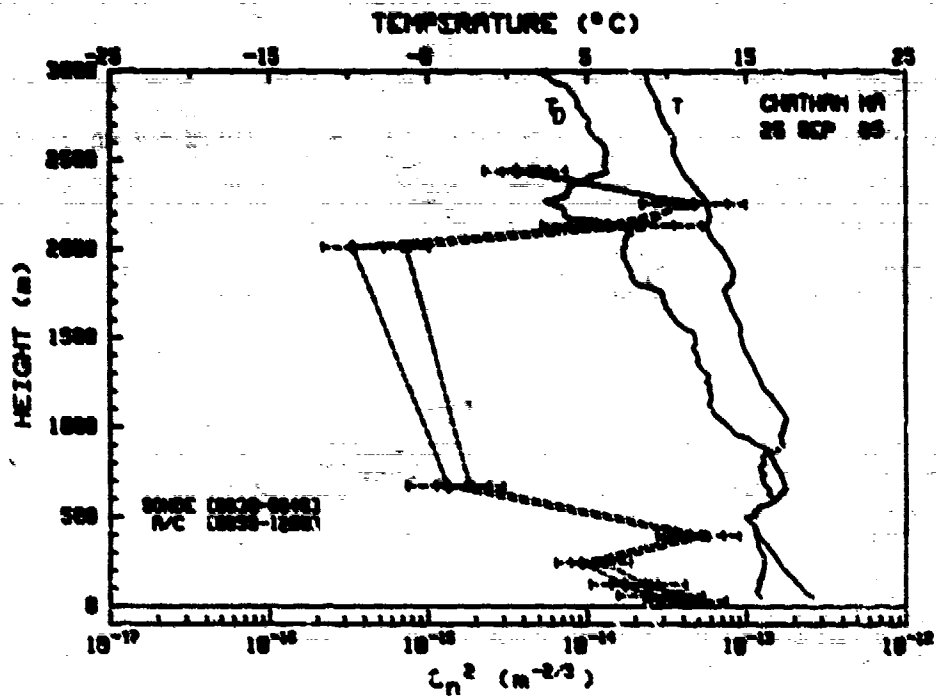


Figure A9. Measured C_n^2 Profile (25 Sept 0959) With T and T_D From Radiosonde Closest in Time

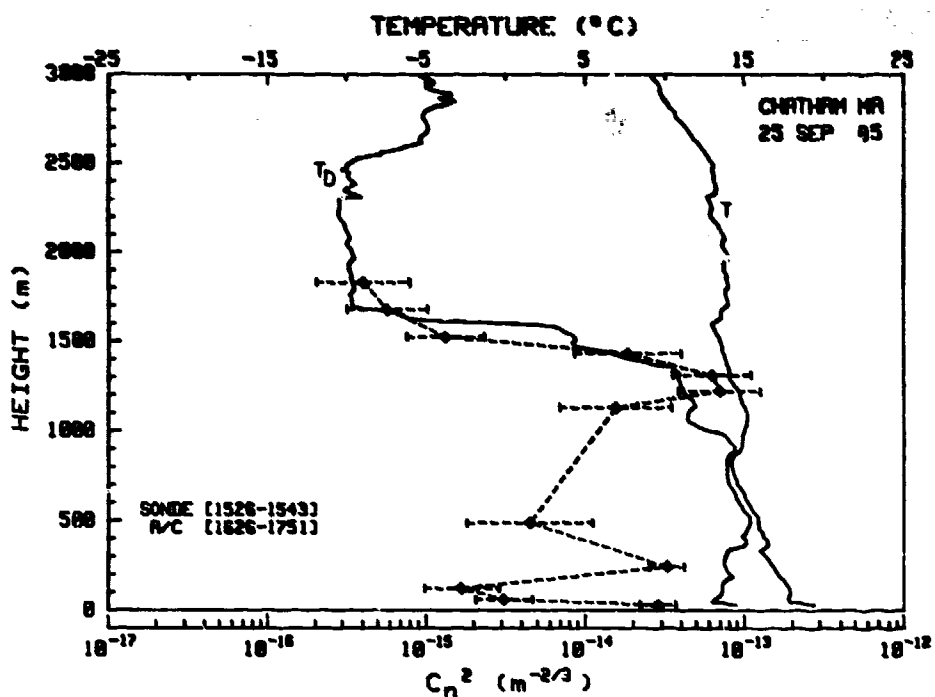


Figure A10. Measured C_n^2 Profile (25 Sept 1626) With T and T_D From Radiosonde Closest in Time

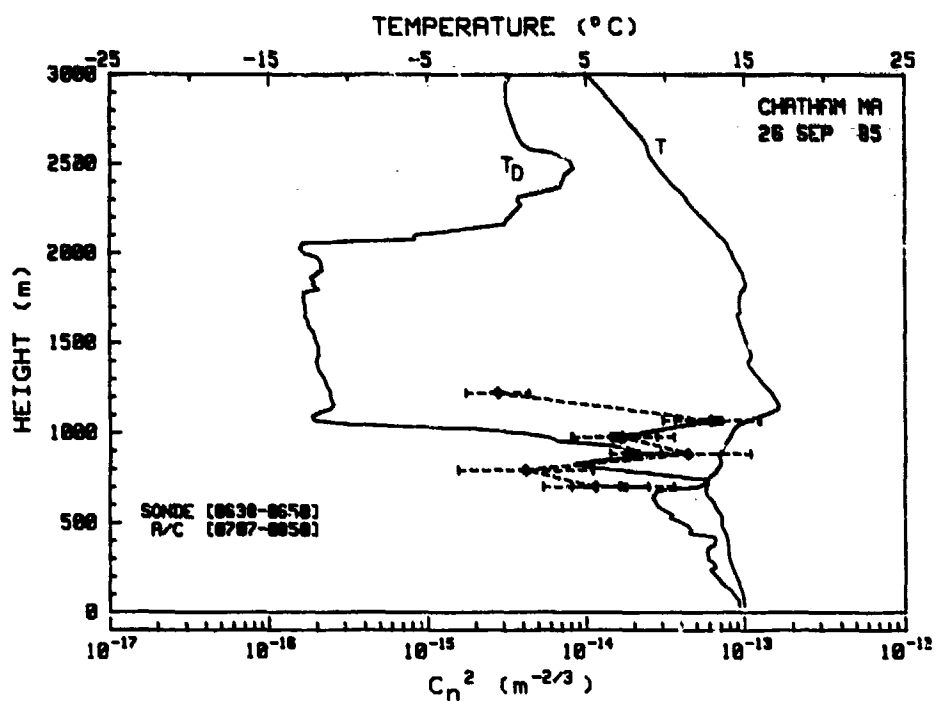


Figure A11. Measured C_n^2 Profile (26 Sept 0707) With T and T_D From Radiosonde

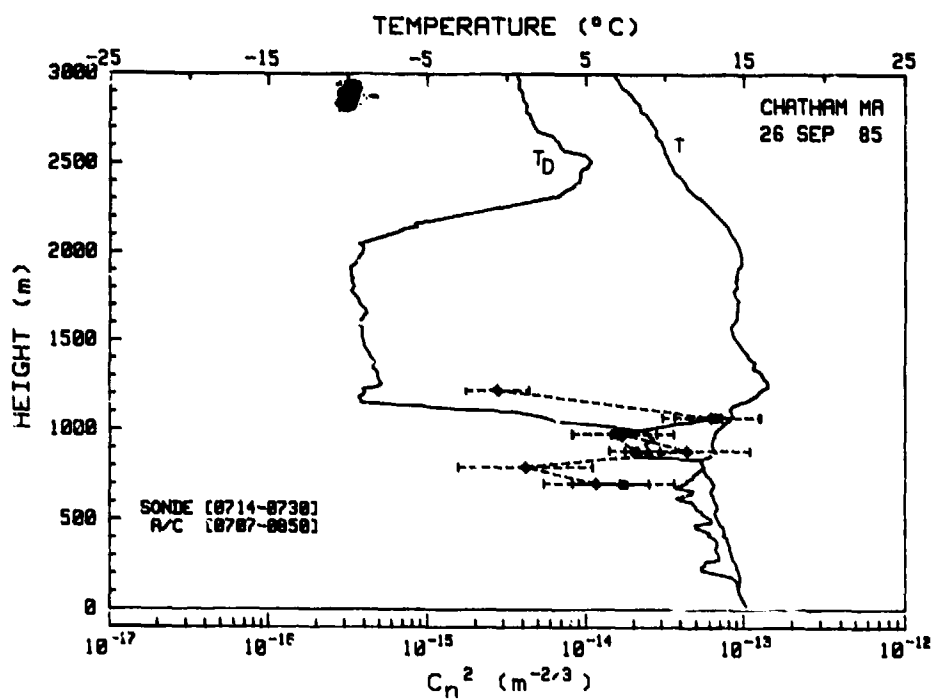


Figure A12. Measured C_n^2 Profile (26 Sept 0707) With T and T_D From Radiosonde Closest in Time

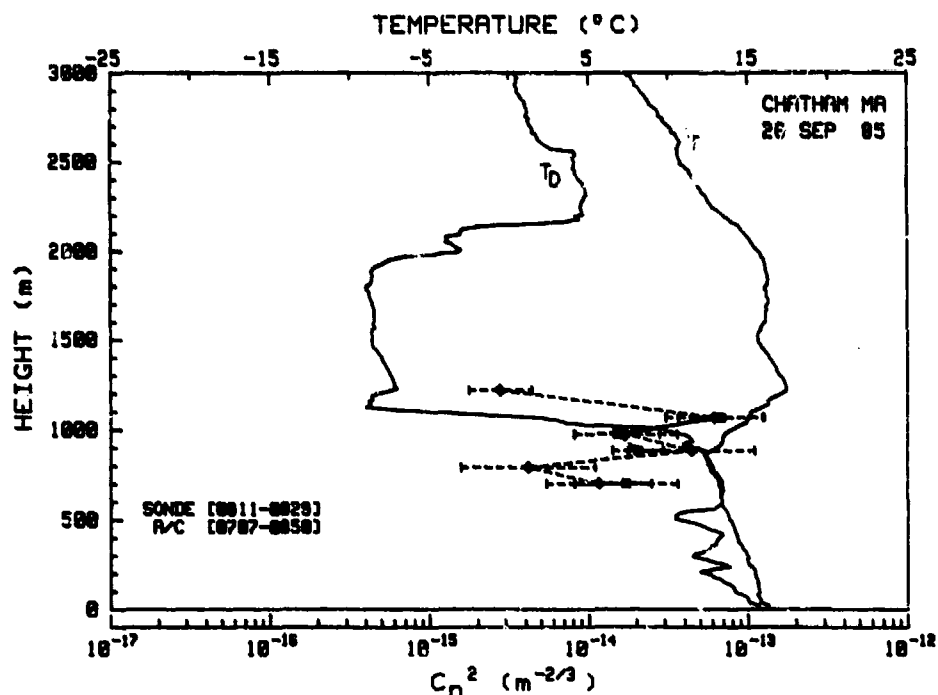


Figure A13. Measured C_n^2 Profile (26 Sept 0707) With T and T_D From Radiosonde

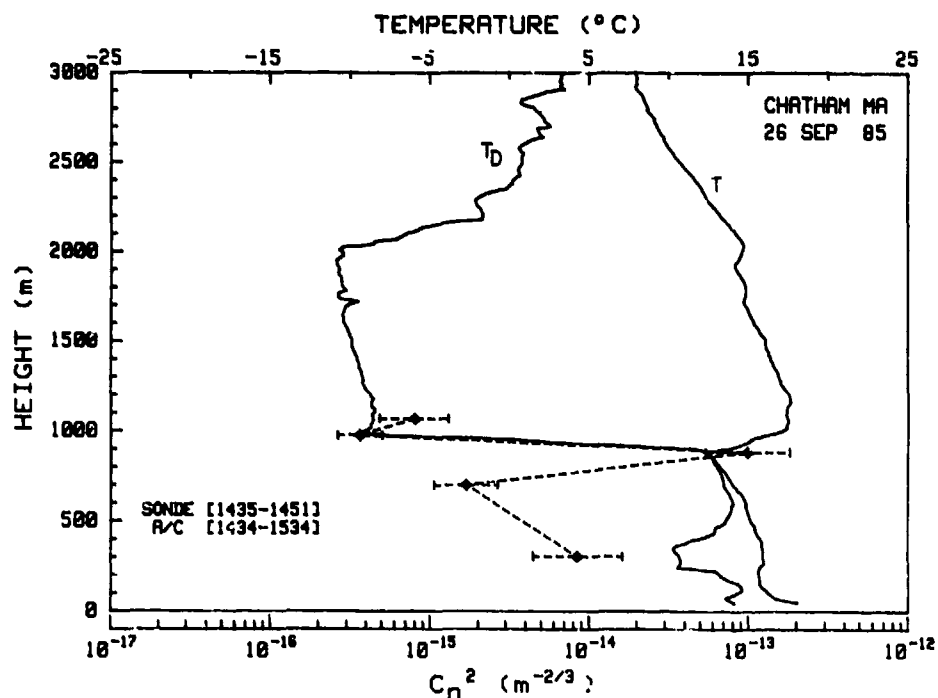


Figure A14. Measured C_n^2 Profile (26 Sept 1434) With T and T_D From Radiosonde Closest in Time